in vivo *37*: 539-547 (2023)
doi:10.21873/invivo.13112

Insulin Docking Within the Open Hemichannel of Connexin 43 May Reduce Risk of Amyotrophic Lateral Sclerosis

STEVEN LEHRER[1] and PETER H. RHEINSTEIN[2]

[1]*Fermata Pharma, New York, NY, U.S.A.;*
[2]*Severn Health Solutions, Severna Park, MD, U.S.A.*

Abstract. *Background/Aim: Type 2 diabetes (T2D), characterized by hyperinsulinemia, protects motor neurons against amyotrophic lateral sclerosis (ALS). Type 1 diabetes and a total lack of insulin are associated with increased risk of ALS. Connexin 43 (Cx43), an astrocyte protein, operates as an open pore via which toxic substances from the astrocytes reach motor neurons. Materials and Methods: In the current study, we performed molecular docking of insulin with monomeric Cx31, monomeric Cx43, and hexameric Cx31 to assess whether insulin might affect the pore. Hexameric Cx31 and hexameric Cx43 are transmembrane hemichannels composed of 6 subunits; they bind together to form gap junction intercellular channels. We used the program AutoDock Vina Extended for the molecular docking study. Results: Cx31 shares amino acid and structural similarity to Cx43, and insulin docks to the same position at the N-terminal domain of monomeric Cx31 and monomeric Cx43. Insulin docks within the open hemichannel of hexameric Cx31, potentially blocking it. Molecular dynamics simulation shows that the block is highly stable and may be responsible for the protective effect of T2D on ALS. Conclusion: Insulin, especially intranasal insulin, might be a treatment for ALS. An insulin secretogogue such as oral sulfonylurea or meglitinide might also be of value.*

Amyotrophic lateral sclerosis (ALS) is a disease of motor neurons that affects up to 30,000 people in the United States each year, with 5,000 new cases being diagnosed. Muscles become weaker over time, affecting physical function, and eventually leading to death. The condition has no single cause and no recognized therapy.

A Danish population-based study indicated that type 2 diabetes (T2D), but not type 1, protected against ALS (1). A Swedish population study identified a significant inverse association between ALS and T2D, but not type 1 diabetes, with the strongest inverse association 6 years after diabetes onset (2). An Italian cohort study revealed a significantly reduced ALS risk in T2D (hazard ratio 0.30) with no effect of sex, age, or ALS phenotype (3). Zhang *et al*. reported that genetically predicted T2D was associated with significantly lower odds of ALS both in European and East Asian populations (4). Type 1 diabetes, characterized by a total lack of insulin, is associated with increased risk of ALS (1, 2).

Connexin 43 (Cx43), an astrocyte protein (also called Gap junction alpha-1 protein, GJA1), operates as an open pore *via* which substances from the astrocytes reach the motor neurons. Patients with ALS who had a family history of the disease and those who had sporadic ALS had the most functional pores and would therefore be most likely to pass toxic substances from astrocytes to motor neurons, producing ALS (5).

Connexin 31 (Cx31) shares amino acid and structural similarity to Cx43 (6, 7). In their hexameric form, both connexins are composed of 6 subunits that function as transmembrane channels. They bind together to form gap junction intercellular channels.

Hyperinsulinemia is a hallmark of T2D (8). In the current study we performed molecular docking of insulin with the Cx43 monomer and Cx31 monomer. We then performed molecular docking of insulin with the Cx31 hexamer (also called Gap junction beta-3 protein, GJB3) to assess whether insulin might affect the pore.

Materials and Methods

We used the program AutoDock Vina Extended for the docking study (9). AutoDock Vina Extended achieves an approximately two orders of magnitude acceleration compared with the molecular docking software AutoDock 4, while also significantly improving the accuracy of the binding mode predictions. Further speed is achieved from parallelism, by using multithreading on multicore

Correspondence to: Dr. Steven Lehrer, Fermata Pharma, 30 West 60th Street, New York, NY, 10023, U.S.A. Tel: +1 2127657132, e-mail: steven@fermatapharma.com

Key Words: Amyotrophic lateral sclerosis, insulin, diabetes.

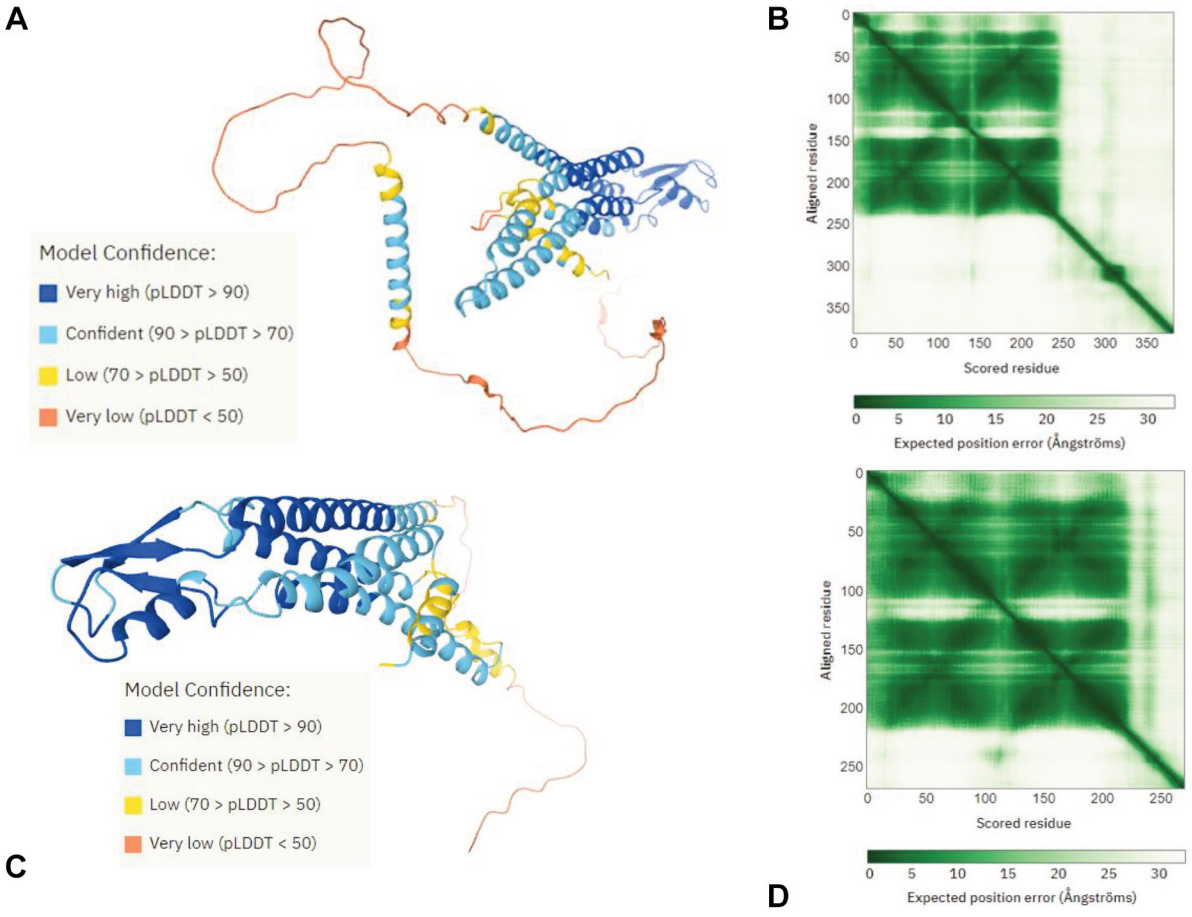

Figure 1. *Structure of Cx43. A) The structure of Cx43 (also called Gap junction alpha-1 protein, GJA1) according to AlphaFold, which produces a per-residue confidence score (pLDDT) between 0 and 100 (lower left). B) Predicted aligned error. The color at position (x, y) indicates AlphaFold's expected position error at residue x, when the predicted and true structures are aligned on residue y. The shade of green indicates expected distance error in Ångströms. The color at (x, y) corresponds to the expected distance error in residue x's position, when the prediction and true structure are aligned on residue y. Dark green is good (low error), light green is bad (high error). C) The structure of Cx31 (also called Gap junction beta-3 protein, GJB3) according to AlphaFold. D) Predicted Cx31 aligned error.*

machines. AutoDock Vina Extended automatically calculates the grid maps and clusters the results in a way transparent to the user. UCSF Chimera 1.14 was used for molecular visualization (10).

The single chain human insulin molecule (humulin B) is from PubChem CID101896409. Human hexameric Cx31 hemichannel in the absence of calcium was deposited in the RCSB Protein Data Bank (6L3T) 2019-10-15, released: 2020-09-09. Human insulin is a heterodimer of an A-chain and a B-chain, which are linked together by disulfide bonds. Heterodimeric human insulin was deposited in the RCSB Protein Data Bank (4EYN) 2012-5-01, released: 2013-05-01.

Cx43 had no entry in the RCBS Protein Data Bank for the complete molecule. We obtained a protein structure prediction for Cx43 (GJA1) from AlphaFold, an artificial intelligence (AI) system developed by Google's DeepMind that predicts a protein's 3D structure from its amino acid sequence. AlphaFold regularly achieves experiment-competitive accuracy (11, 12).

Cx31 had no entry in the RCBS Protein Data Bank for the monomer. We obtained a monomeric protein structure prediction for Cx31 (GJB3) from AlphaFold. We used the ClusPro Server for protein-protein docking of human insulin (4EYN) to the Cx31 hexamer. ClusPro (https://cluspro.org) is a widely used tool for protein–protein docking. The server provides a simple home page for basic use, requiring only two files in Protein Data Bank (PDB) format (13). The quality of automated docking by ClusPro is very close to that of the best human predictor groups (14).

We used GROMACS to perform molecular dynamics simulation of the human insulin (4EYN) docked to the Cx31 hexamer. GROMACS is a molecular dynamics package mainly designed for simulations of proteins, lipids, and nucleic acids.

Results

Figure 1A shows the structure of Cx43 according to AlphaFold, which produces a per-residue confidence score (pLDDT) between 0 and 100. Figure 1B displays predicted aligned error in Alpha Fold. Figure 1C shows the structure

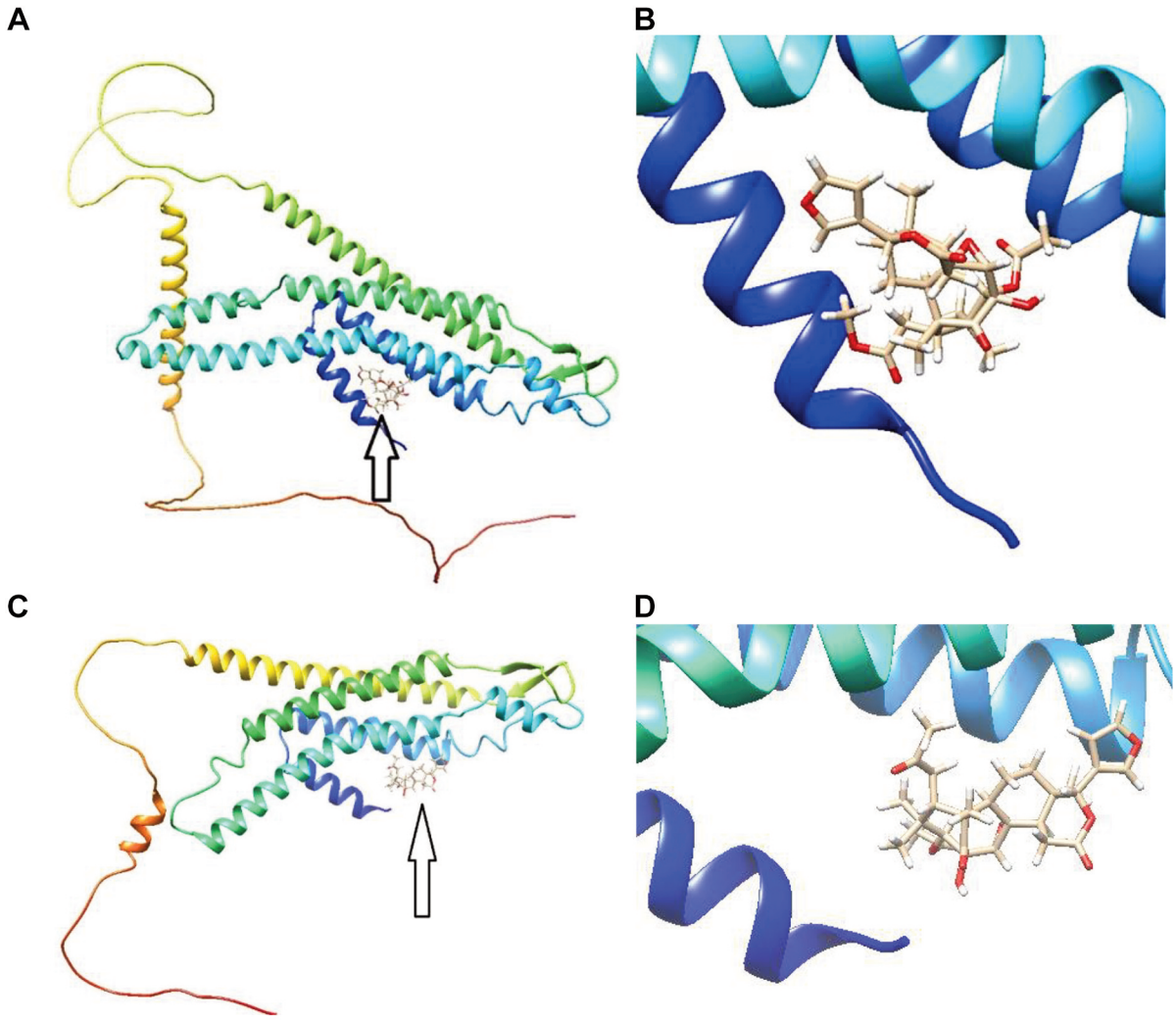

Figure 2. *Insulin docking to human Cx43. A) Human Cx43 in its monomeric form docked with humulin B single chain insulin molecule at the Cx43 N-terminal domain. Arrow indicates the insulin molecule. B) Closeup of Cx43 docked to insulin molecule. Per residue confidence score (pLDDT) from AlphaFold of the N-terminal domain is confident, 90 <pLDDT >70. In other words, we are 70%-90% confident that the N-terminal domain structure is correct. C) Human Cx31 in its monomeric form docked with insulin at the Cx31 N-terminal domain. Arrow indicates the insulin molecule. D) Closeup of Cx31 docked to insulin molecule. Per residue confidence score (pLDDT) from AlphaFold of the N-terminal domain (C) is confident, 90 <pLDDT >70. In other words, we are 70%-90% confident that the N-terminal domain structure is correct. Note that insulin docks to almost the identical position in monomeric Cx31 and monomeric Cx43.*

of CX31 according AlphaFold. Figure 1D displays Cx31 predicted aligned error in Alpha Fold.

The structure of human Cx43 in its monomeric form docked with insulin is shown in Figure 2A. Arrows indicate the insulin molecule docked to the Cx43 N-terminal domain. Figure 2B is a closeup of the docked insulin molecule. Figure 2C shows human Cx31 in its monomeric form docked with insulin. Arrows indicate the insulin molecule docked to the Cx31 N-terminal domain. Figure 2D is a closeup of the docked insulin molecule. Insulin docks to almost the identical position in monomeric Cx31 and monomeric Cx43.

Figure 3 illustrates the binding affinities (kcal/mol) calculated for 10 docking sites of insulin to monomeric Cx43. Only the site with the highest affinity (upper left in figure) was a valid position. Table I contains docking parameters of insulin to monomeric Cx43 calculated by AutoDock Vina Extended. Lower values of root-mean-square deviations of atomic positions (RMSD) indicate that docking is validated with higher accuracy. RMSD values of 3 or more indicate no docking. One docking position, mode 1, with RMSD=0 is highly valid.

The binding affinities (kcal/mol) calculated for 10 docking sites of insulin to monomeric Cx31 is shown in Figure 4.

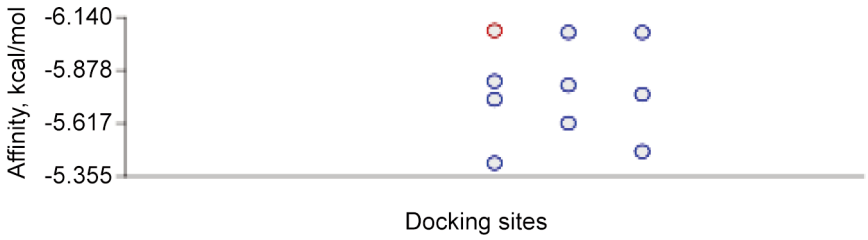

Figure 3. *Binding affinities (kcal/mol) calculated for 10 docking sites of insulin to monomeric Cx43. Only one site with the highest affinity (upper left) was a valid position.*

Table I. *Docking parameters calculated using AutoDock Vina Extended for human monomeric Cx43 to insulin. Lower values of root-mean-square deviations of atomic positions (RMSD) indicate that docking is validated with higher accuracy. RMSD values of 3 or more indicate no docking has occurred. One docking position, mode 1, with RMSD=0 is highly valid.*

Mode	Affinity (kcal/mol)	Ki (μmol)	RMSD lower bound (Å)	RMSD upper bound (Å)
1	–6.074602412	35.26029	0	0
2	–6.065978959	35.77725	27.73112185	31.15029382
3	–6.065369451	35.81407	2.902005898	8.116629233
4	–5.824558059	53.77367	1.92658046	7.437705569
5	–5.805591846	55.52288	2.733718603	8.206586658
6	–5.759997329	59.96433	2.771359767	8.194987559
7	–5.735407323	62.50541	2.208205522	5.237036912
8	–5.617848751	76.22346	2.149206141	7.494382604
9	–5.477866589	96.53755	15.877928	19.02405307
10	–5.420853417	106.2887	2.428831289	5.403085509

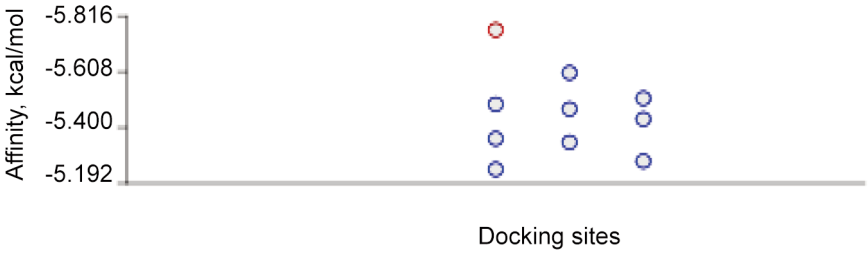

Figure 4. *Binding affinities (kcal/mol) calculated for 10 docking sites of insulin to monomeric Cx31. Only one site with the highest affinity (upper left) was a valid position.*

Only the site with the highest affinity (upper left) was a valid position. Table II contains docking parameters of insulin to monomeric Cx31 calculated by AutoDock Vina Extended. One docking position, mode 1, with RMSD=0 is highly valid. The binding affinities (kcal/mol) calculated for 10 docking sites of insulin to hexameric Cx31 are shown in Figure 5. Only the hemichannel site with the highest affinity (upper left in figure) was a valid position. Figure 6A shows human Cx31 in its hexameric form docked with insulin. Arrows indicate the insulin molecule docked within the hemichannel. Figure 6B is a closeup of the docked insulin molecule. Table III contains docking parameters of insulin to hexameric Cx31 calculated by AutoDock Vina Extended. One docking position, mode 1, with RMSD=0 is highly valid.

Figure 7A shows the structure of human insulin (4EYN) as a heterodimer of A-chain (left) and B-chain (right). Figure 7B shows human Cx31 in its hexameric form with the open hemichannel (center) docked with human insulin using the ClusPro Server. Note that the human insulin heterodimer completely blocks the open hemichannel.

Figure 8 shows the first six configurations (clusters) of human Cx31 in its hexameric form with the open hemichannel docked with human insulin according to ClusPro. Configuration 0, the highest ranked, is shown

Table II. *Docking parameters calculated using AutoDock Vina Extended for human monomeric Cx43 to insulin. Lower values of root-mean-square deviations of atomic positions (RMSD) indicate that docking is validated with higher accuracy. RMSD values of 3 or more indicate no docking has occurred. One docking position, mode 1, with RMSD=0 is highly valid.*

Mode	Affinity (kcal/mol)	Ki (μmol)	RMSD lower bound (Å)	RMSD upper bound (Å)
1	–5.764226326	59.53785	0	0
2	–5.604354028	77.97948	20.29215496	24.5788459
3	–5.50895568	91.6026	24.13479769	26.64546373
4	–5.487040562	95.05428	24.10361311	28.26772351
5	–5.469198364	97.9603	25.81208942	28.4784468
6	–5.431554356	104.3863	19.49592317	23.8544476
7	–5.358509811	118.0825	3.708488437	4.594993627
8	–5.344926538	120.8209	24.15928651	26.64988346
9	–5.274514921	136.0674	25.04492059	29.83058177
10	–5.244106707	143.2331	25.62035767	28.69788407

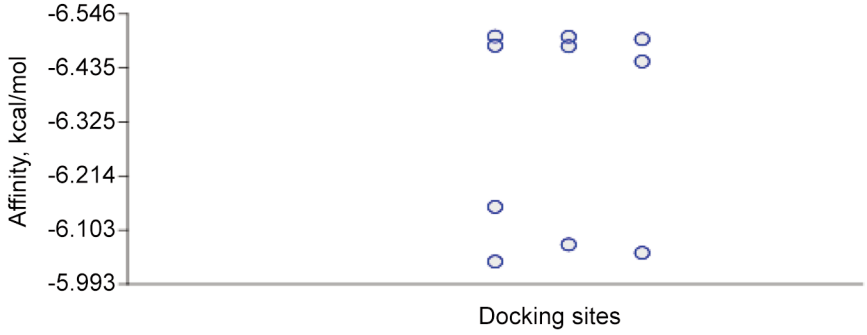

Figure 5. *Binding affinities (kcal/mol) calculated for 10 docking sites of humulin B insulin to Cx31 hexamer. Only one site with the highest affinity (upper left) was a valid position.*

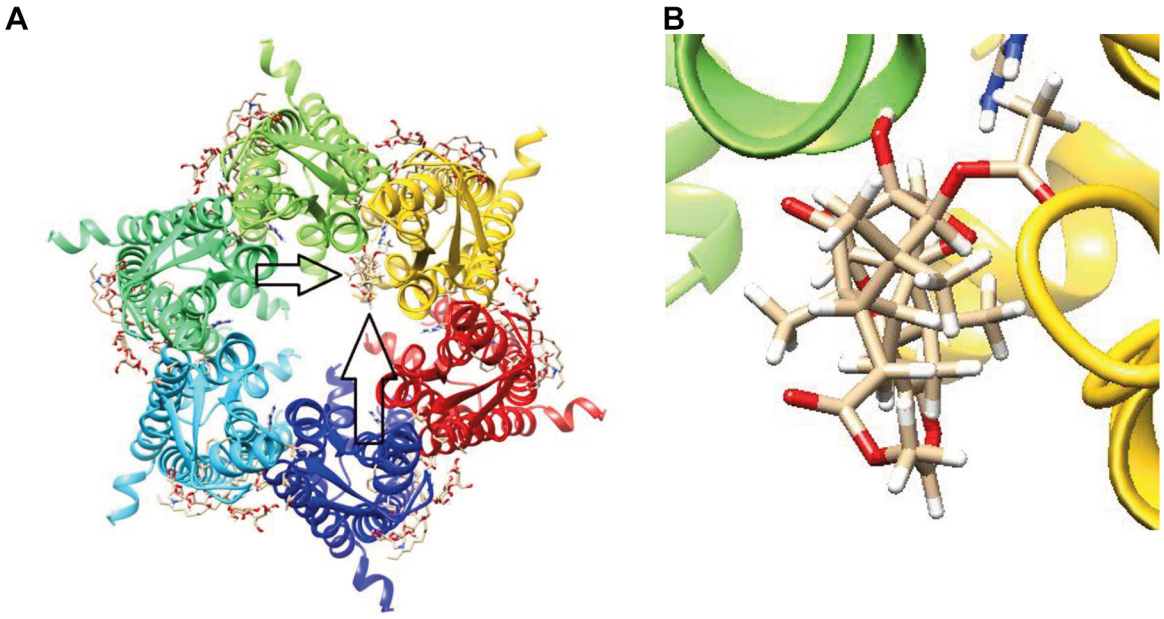

Figure 6. *Human Cx31 docked with insulin. A) Human Cx31 in its hexameric form with open hemichannel (center) docked with humulin B single chain insulin molecule. Arrows indicate the insulin molecule within the hemichannel. B) Closeup of docked humulin B, single chain insulin molecule.*

Table III. *Docking parameters calculated using AutoDock Vina Extended of hexameric Cx31 to insulin. One docking position, mode 1, with RMSD=0 is highly valid.*

Mode	Affinity (kcal/mol)	Ki (μmol)	RMSD lower bound (Å)	RMSD upper bound (Å)
1	–6.499765043	17.2044	0	0
2	–6.498996353	17.22674	8.738951896	10.75563818
3	–6.49403788	17.37151	16.04060202	18.62194177
4	–6.480787951	17.76437	8.710319846	10.73125405
5	–6.479632275	17.79906	18.41293941	21.47099771
6	–6.448499272	18.75934	16.05073372	18.60996308
7	–6.150886428	31.00055	28.43659168	33.35036486
8	–6.073789675	35.30869	22.76797584	26.71361825
9	–6.056759246	36.33834	34.99424228	38.79479813
10	–6.038860805	37.45283	40.62664359	44.9530327

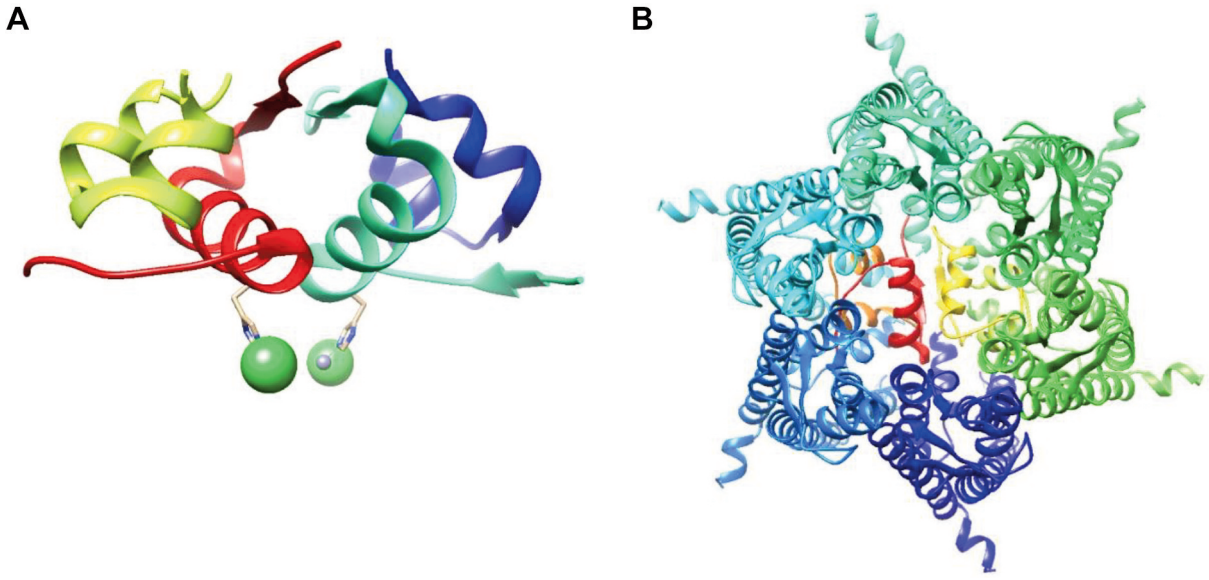

Figure 7. *Human insulin heterodimer in Cx43 hemichannel. A) The structure of the human insulin (RCBS Protein Data Bank 4EYN) as the heterodimer of A-chain (left) and B-chain (right). B) Human Cx31 in its hexameric form with open hemichannel (center) docked with human insulin in the highest ranked ClusPro configuration. Note that the human insulin heterodimer completely blocks the open hemichannel (center).*

enlarged and rotated in Figure 7B. Note that the human insulin heterodimer (red) is in the identical position in all six configurations, blocking the open Cx31 hemichannel.

Table IV lists cluster scores and energies for Human Cx31 in its hexameric form with the open hemichannel docked with human insulin heterodimer. The ligand position with the most *neighbors* within 9 angstroms becomes a cluster center, and its neighbors the members of the cluster. These were then removed from the set and a second cluster center was located, then a third, up to cluster 5. Thus, the cluster rank was determined.

Figure 9 is a molecular dynamics simulation of human Cx31 in its hexameric form with the open hemichannel docked with human insulin heterodimer. Time series shows the RMSD levels fluctuation ~0.1 nm (1 Å), indicating that the structure is quite stable. The reasonably invariant radius of gyration (Rg) values indicate that the docked protein remains highly stable over the course of 1 ns. These results suggest that once insulin blocks the Cx31 open hemichannel, the block is stable and will remain in place.

Discussion

Cx43 is normally expressed in astrocytes and found in most human astrocytomas and in the astroglial component of glioneuronal tumors (15). Astrocytes may induce the death

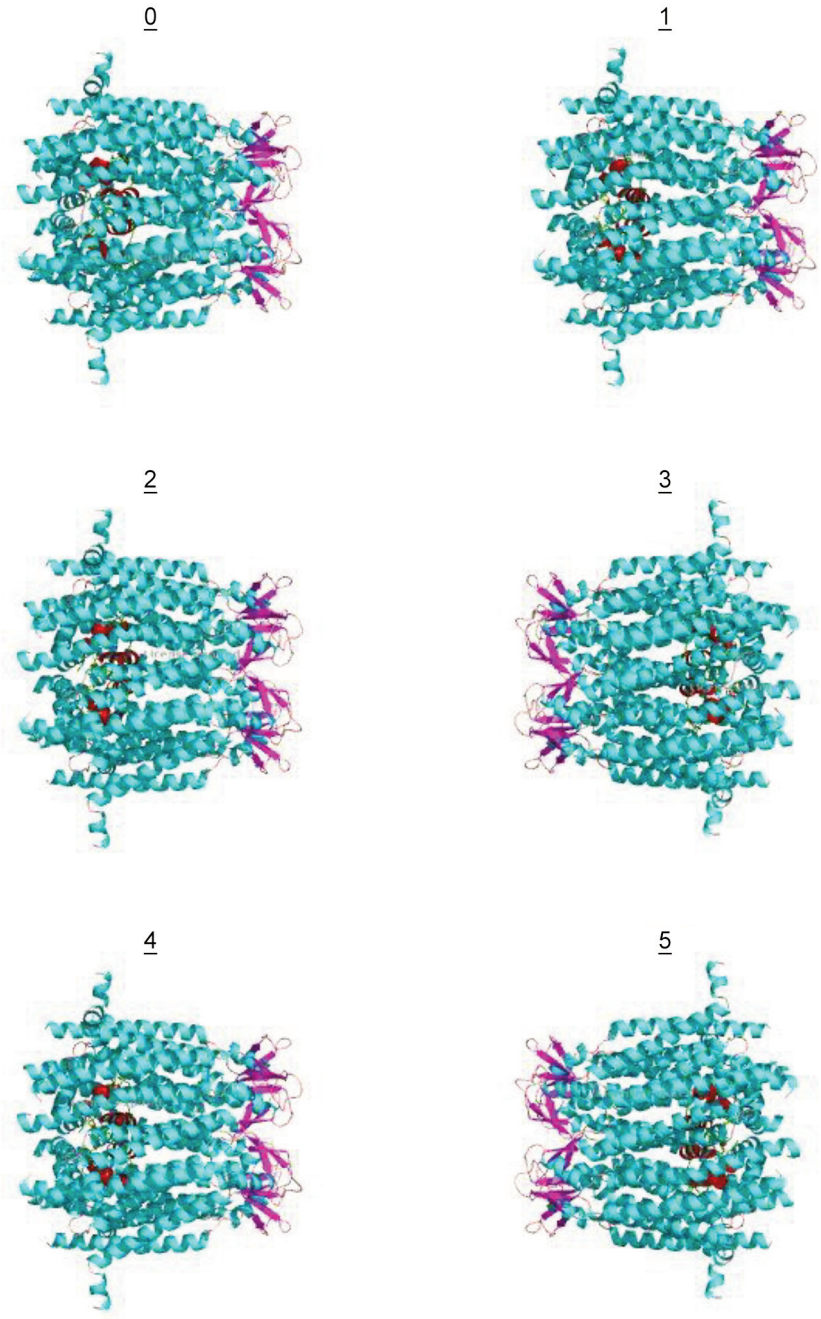

Figure 8. *The results from ClusPro showing the first six configurations (clusters) of Human Cx31 in its hexameric form with the open hemichannel docked with human insulin. Configuration 0, the highest ranked, is shown enlarged and rotated in figure 7B. Note that the human insulin heterodimer (red) is in the identical position in all six configurations, blocking the open Cx31 hemichannel.*

of motor neurons since astrocyte dysfunction occurs after symptom onset in patients with ALS. Astrocytes provoke motor neuron death through Cx43 hemichannels that allow the movement of toxic astrocyte substances into motor neurons. Cx43 protein is elevated in the cerebrospinal fluid of ALS patients and could be a biomarker (5).

Because astrocytes may be responsible for the progression of ALS, drugs that block Cx43 hemichannels might be therapeutic (5). One analysis of the Cx43 structure revealed a closed sieve-like molecular gate (16). The Cx43 N-terminal domain is involved in channel gating and oligomerization and may control the switch between the channel's open and

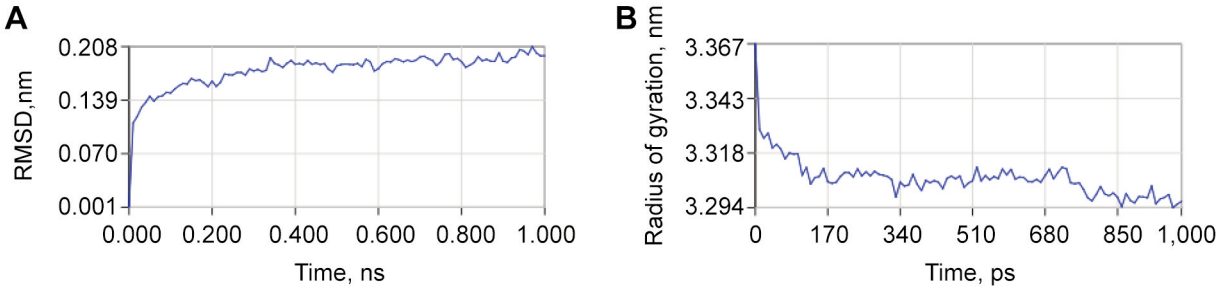

Figure 9. *Molecular dynamics simulation of human insulin in Cx31 hemichannel. A) Molecular dynamics simulation human Cx31 in its hexameric form with the open hemichannel docked with human insulin heterodimer. Time series shows the RMSD levels fluctuation of ~0.1 nm (1 Å), indicating that the structure is quite stable. B) Radius of gyration (Rg). The reasonably invariant Rg values indicate that the docked protein remains highly stable over the course of 1 ns. These results suggest that once insulin blocks the Cx31 open hemichannel, the block is stable and will remain in place.*

closed states. Therefore, the docking of insulin to the Cx43 N-terminal domain we demonstrate here may be capable of blocking the channel, preventing toxic astrocyte substances from entering and destroying motor neurons.

Our finding that insulin docks within the open hemichannel of hexameric Cx31, potentially blocking it, again suggests that the block may be responsible for the inverse relationship between ALS and T2D. This conclusion is reinforced by the fact that insulin docks to the same position, the N-terminal domain, of monomeric Cx31 and monomeric Cx43 (Figure 2). Molecular dynamics simulation indicates that once insulin blocks the Cx31 open hemichannel, the block is stable and will remain in place. Therefore, insulin might be a treatment for ALS, especially since insulin enhances glucose-stimulated insulin secretion in healthy humans (17). Type 1 diabetes, characterized by a total lack of insulin, is associated with increased risk of ALS (1, 2), again suggesting that insulin could have a beneficial effect on ALS.

Therapeutic insulin would likely need to be administered intranasally, rather than parenterally, to achieve an adequate dose to the cerebrospinal fluid (CSF). CSF insulin levels are normally much lower than plasma insulin levels (18). Normal plasma insulin is 50 pmol/l compared to 3.3 pmol/l in normal CSF (19). Intranasal insulin achieves direct access to the CSF within 30 minutes, bypassing the bloodstream (20). Insulin secretogogues such as oral sulfonylurea or meglitinide might also be of value.

However, this hypothesis has several weaknesses. Zhang *et al*. did not observe a significant association between 2 h glucose, fasting glucose, fasting insulin, fasting proinsulin, HbA1C and the risk of ALS in European populations (4). However, Zhang *et al*. measured fluctuations in plasma insulin that may have been related to much smaller changes in CSF insulin, given that low CSF insulin levels are normally observed (19). Moreover, the Cx43 gene, GJA1, has multiple polymorphisms, and some may affect Cx43 interaction with insulin (21). Furthermore, insulin docks almost identically within monomeric Cx31 and monomeric Cx43. We assume that insulin docks identically within hexameric Cx31 and hexameric Cx43, but this may not be the case. Cx31 abnormalities are associated with erythrokeratoderma, a rare skin condition (22).

Table IV. *Cluster scores and energies for Human Cx31 in its hexameric form with the open hemichannel docked with human insulin heterodimer. The ligand position with the most neighbors within 9 angstroms becomes a cluster center, and its neighbors the members of the cluster. These are then removed from the set and a second cluster center is located, then a third, up to cluster 5. Thus, the cluster rank is determined.*

Cluster	Members	Representative	Weighted score
0	129	Center	–1,627.9
0	129	Lowest energy	–2,103.9
1	127	Center	–1,732.6
1	127	Lowest energy	–2,166
2	126	Center	–1,688.6
2	126	Lowest energy	–2,073.5
3	122	Center	–1,636.6
3	122	Lowest energy	–2,119.6
4	120	Center	–1,690.2
4	120	Lowest energy	–2,104
5	111	Center	–1,733.9
5	111	Lowest energy	–2,109.6

In summary, the docking results presented here indicate that insulin may be capable of inhibiting the progression of ALS by blocking Cx43 hemichannels. Further study is warranted.

Conflicts of Interest

The Authors have no conflicts of interest to declare in relation to this study.

Authors' Contributions

Dr. Lehrer and Dr. Rheinstein contributed equally to the conception, writing, and data analysis of this study.

References

1 Kioumourtzoglou MA, Rotem RS, Seals RM, Gredal O, Hansen J and Weisskopf MG: Diabetes mellitus, obesity, and diagnosis of amyotrophic lateral sclerosis: a population-based study. JAMA Neurol *72(8)*: 905-911, 2015. PMID: 26030836. DOI: 10.1001/jamaneurol.2015.0910

2 Mariosa D, Kamel F, Bellocco R, Ye W and Fang F: Association between diabetes and amyotrophic lateral sclerosis in Sweden. Eur J Neurol *22(11)*: 1436-1442, 2015. PMID: 25600257. DOI: 10.1111/ene.12632

3 D'Ovidio F, d'Errico A, Carnà P, Calvo A, Costa G and Chiò A: The role of pre-morbid diabetes on developing amyotrophic lateral sclerosis. Eur J Neurol *25(1)*: 164-170, 2018. PMID: 28921834. DOI: 10.1111/ene.13465

4 Zhang L, Tang L, Huang T and Fan D: Association between type 2 diabetes and amyotrophic lateral sclerosis. Sci Rep *12(1)*: 2544, 2022. PMID: 35169211. DOI: 10.1038/s41598-022-06463-6

5 Almad AA, Taga A, Joseph J, Gross SK, Welsh C, Patankar A, Richard JP, Rust K, Pokharel A, Plott C, Lillo M, Dastgheyb R, Eggan K, Haughey N, Contreras JE and Maragakis NJ: Cx43 hemichannels contribute to astrocyte-mediated toxicity in sporadic and familial ALS. Proc Natl Acad Sci U.S.A. *119(13)*: e2107391119, 2022. PMID: 35312356. DOI: 10.1073/pnas.2107391119

6 Hawat G and Baroudi G: Connexin 43 hemichannels and pharmacotherapy of myocardial ischemia injury. Novel Strategies in Ischemic Heart Disease: 189-218, 2016. DOI: 10.5772/32201

7 Lee HJ, Jeong H, Hyun J, Ryu B, Park K, Lim HH, Yoo J and Woo JS: Cryo-EM structure of human Cx31.3/GJC3 connexin hemichannel. Sci Adv *6(35)*: eaba4996, 2020. PMID: 32923625. DOI: 10.1126/sciadv.aba4996

8 Weyer C, Hanson RL, Tataranni PA, Bogardus C and Pratley RE: A high fasting plasma insulin concentration predicts type 2 diabetes independent of insulin resistance: evidence for a pathogenic role of relative hyperinsulinemia. Diabetes *49(12)*: 2094-2101, 2000. PMID: 11118012. DOI: 10.2337/diabetes.49.12.2094

9 Trott O and Olson AJ: AutoDock Vina: improving the speed and accuracy of docking with a new scoring function, efficient optimization, and multithreading. J Comput Chem *31(2)*: 455-461, 2010. PMID: 19499576. DOI: 10.1002/jcc.21334

10 Pettersen EF, Goddard TD, Huang CC, Couch GS, Greenblatt DM, Meng EC and Ferrin TE: UCSF Chimera—a visualization system for exploratory research and analysis. J Comput Chem *25(13)*: 1605-1612, 2004. PMID: 15264254. DOI: 10.1002/jcc.20084

11 Jumper J, Evans R, Pritzel A, Green T, Figurnov M, Ronneberger O, Tunyasuvunakool K, Bates R, Žídek A, Potapenko A, Bridgland A, Meyer C, Kohl SAA, Ballard AJ, Cowie A, Romera-Paredes B, Nikolov S, Jain R, Adler J, Back T, Petersen S, Reiman D, Clancy E, Zielinski M, Steinegger M, Pacholska M, Berghammer T, Bodenstein S, Silver D, Vinyals O, Senior AW, Kavukcuoglu K, Kohli P and Hassabis D: Highly accurate protein structure prediction with AlphaFold. Nature *596(7873)*: 583-589, 2021. PMID: 34265844. DOI: 10.1038/s41586-021-03819-2

12 Komaroff AL: Breakthrough discovery in protein structure prediction and the promise of new treatments. JAMA *326(14)*: 1369-1370, 2021. PMID: 34554183. DOI: 10.1001/jama.2021.15728

13 Kozakov D, Hall DR, Xia B, Porter KA, Padhorny D, Yueh C, Beglov D and Vajda S: The ClusPro web server for protein-protein docking. Nat Protoc *12(2)*: 255-278, 2017. PMID: 28079879. DOI: 10.1038/nprot.2016.169

14 Kozakov D, Beglov D, Bohnuud T, Mottarella SE, Xia B, Hall DR and Vajda S: How good is automated protein docking? Proteins *81(12)*: 2159-2166, 2013. PMID: 23996272. DOI: 10.1002/prot.24403

15 Aronica E, Gorter JA, Jansen GH, Leenstra S, Yankaya B and Troost D: Expression of connexin 43 and connexin 32 gap-junction proteins in epilepsy-associated brain tumors and in the perilesional epileptic cortex. Acta Neuropathol *101(5)*: 449-459, 2001. PMID: 11484816. DOI: 10.1007/s004010000305

16 Qi C, Acosta-Gutierrez S, Lavriha P, Othman A, Lopez-Pigozzi D, Bayraktar E, Schuster D, Picotti P, Zamboni N and Bortolozzi M: Structure of the connexin-43 gap junction channel reveals a closed sieve-like molecular gate. bioRxiv, 2022. DOI: 10.1101/2022.03.26.485947

17 Bouche C, Lopez X, Fleischman A, Cypess AM, O'Shea S, Stefanovski D, Bergman RN, Rogatsky E, Stein DT, Kahn CR, Kulkarni RN and Goldfine AB: Insulin enhances glucose-stimulated insulin secretion in healthy humans. Proc Natl Acad Sci U.S.A. *107(10)*: 4770-4775, 2010. PMID: 20176932. DOI: 10.1073/pnas.1000002107

18 Born J, Lange T, Kern W, Mcgregor G, Bickel U and Fehm H: Sniffing neuropeptides: a transnasal approach to the human brain. Nature Neuroscience *5(6)*: 514-516, 2021. DOI: 10.1038/nn0602-849

19 Craft S, Peskind E, Schwartz MW, Schellenberg GD, Raskind M and Porte D Jr: Cerebrospinal fluid and plasma insulin levels in Alzheimer's disease: relationship to severity of dementia and apolipoprotein E genotype. Neurology *50(1)*: 164-168, 1998. PMID: 9443474. DOI: 10.1212/wnl.50.1.164

20 Hallschmid M: Intranasal insulin. J Neuroendocrinol *33(4)*: e12934, 2021. PMID: 33506526. DOI: 10.1111/jne.12934

21 Zhang J, You Q, Shu J, Gang Q, Jin H, Yu M, Sun W, Zhang W and Huang Y: GJA1 gene polymorphisms and topographic distribution of Cranial MRI lesions in cerebral small vessel Disease. Front Neurol *11*: 583974, 2020. PMID: 33324328. DOI: 10.3389/fneur.2020.583974

22 Charfeddine C, Laroussi N, Mkaouar R, Jouini R, Khayat O, Redissi A, Mosbah A, Dallali H, Chedly Debbiche A, Zaouak A, Fenniche S, Abdelhak S and Hammami-Ghorbel H: Expanding the clinical phenotype associated with NIPAL4 mutation: Study of a Tunisian consanguineous family with erythrokeratodermia variabilis-Like Autosomal Recessive Congenital Ichthyosis. PLoS One *16(10)*: e0258777, 2021. PMID: 34669720. DOI: 10.1371/journal.pone.0258777

Received December 24, 2022
Revised January 4, 2023
Accepted January 5, 2023